

Institut für Kunststofftechnologie der Universität Stuttgart

Prediction of primary normal stress difference from shear viscosity data using a single integral constitutive equation

M. H. Wagner

With 9 figures and 2 tables

(Received December 3, 1976)

1. Introduction

Ever since *Weissenberg* demonstrated the presence of normal stresses in steady shear flow of elastic liquids (1), great interest has been expressed in both the experimental and theoretical aspects of these phenomena. It is well known that three independent stress functions, which are usually taken to be the shear stress τ_{12} , and the first and second normal stress differences, σ_1 and σ_2 , respectively, are sufficient to characterize the steady shear flow of "simple" incompressible fluids (2). Correlations between these three stress functions are obtained by more specific constitutive assumptions, which can be tested on their usefulness by comparing theoretical predictions with experimental evidence.

In two recent papers by *Bird et al.* (3, 4), a relation between the steady state values of the primary normal stress function θ ,

$$\theta = \frac{\sigma_1}{\dot{\gamma}^2} = \frac{\tau_{11} - \tau_{22}}{\dot{\gamma}^2}, \quad [1]$$

and the viscosity function η ,

$$\eta = \frac{\tau_{12}}{\dot{\gamma}}, \quad [2]$$

was proposed, which was based on the *Goddard-Miller* rheological equation of state (5), and which was of the general *Kramers-Kronig* type (6):

$$\theta(\dot{\gamma}) = \frac{4}{\pi} \int_0^{\infty} \frac{\eta(\dot{\gamma}') - \eta(\dot{\gamma})}{\dot{\gamma}'^2 - \dot{\gamma}^2} d\dot{\gamma}'. \quad [3]$$

This relation was compared with the viscosity and primary normal stress data of six polymer melts, three polymer solutions, and an aluminium soap solution, which were measured

by several research groups (7–11) and are available in the literature. Agreement between predicted and measured values of the primary normal stress function was reasonable, provided that the right hand side of eq. [3] was multiplied by a purely empirical front factor K . It was found that K has to be taken 3 for polymer melts and 2 for solutions.

In this paper, a different relation between the primary normal stress function θ and the viscosity function η is presented,

$$\theta(\dot{\gamma}) = -\frac{1}{n} \frac{d\eta(\dot{\gamma})}{d\dot{\gamma}}, \quad [4]$$

which results from a BKZ-type (i.e. strain-dependent) single integral constitutive equation. According to this theory, the primary normal stress function θ can be obtained from viscosity data by simple differentiation with respect to the shear rate $\dot{\gamma}$. The material parameter n is associated with the strain dependence of the memory function. This constitutive equation has already been successfully used (12) in describing the time-dependent non-linear shear stress and first normal stress difference behavior of a well characterized low-density polyethylene melt at constant strain rate as observed by *Meissner* (13, 14).

Here, the same set of data as used by *Bird et al.* (3, 4) will be taken, and it will be shown that eq. [4] is a valid description of material behavior in spite of the vast differences in physical constitution and chemical structure of the polymer melts and solutions considered.

2. Constitutive equation

A widely used class of integral theories (15–18) has the general form

$$\tau = \int_0^{\infty} [m_1(s, I_1, I_2) C_t^{-1} + m_2(s, I_1, I_2) C_t] ds, \quad [5]$$

where C_t^{-1} and C_t are the *Finger* and *Cauchy* tensor respectively, and the memory functions m_1 and m_2 are assumed to be functions of the time difference s and the first and second invariant of the *Finger* tensor.

As the secondary normal stress difference is not considered here, m_2 is set equal to zero. The further assumption was made (12) that m_1 is expressible as a product of two functions,

$$m_1(s, I_1, I_2) = \mu(s)h(I_1, I_2), \quad [6]$$

where $h(I_1, I_2)$, which was called the damping function, tends to unity for small deformations, and $\mu(s)$ is identical with the rubberlike-liquid memory function, to be determined from linear viscoelastic data (19–23).

For stress growth at inception of steady flow, i.e. for the case of zero deformation rate for times $t < 0$ and constant deformation rate for times $t \geq 0$, eq. [5] leads to

$$\tau = \int_0^t \mu(s)h(I_1, I_2) C_t^{-1}(t-s) ds + h(I_1, I_2) C_t^{-1}(0) \int_t^{\infty} \mu(s) ds. \quad [7]$$

Using integration by parts, eq. [7] can be rearranged to

$$\tau = \int_0^t G(s)h(I_1, I_2) C_t^{-1}(t-s) \cdot \left[\frac{\partial}{\partial s} \ln(h(I_1, I_2) \cdot C_t^{-1}(t-s)) \right] ds, \quad [8]$$

where the relaxation modulus of linear viscoelasticity, $G(t)$, is equal to the time integral of the memory function $\mu(t)$

$$G(t) = \int_t^{\infty} \mu(s) ds. \quad [9]$$

The *Finger* tensor $C_t^{-1}(t')$ for steady shear flow at constant shear rate $\dot{\gamma}$ and constant volume is given by

$$C_t^{-1}(t') = \begin{vmatrix} 1 + \dot{\gamma}^2(t-t')^2 & \dot{\gamma}(t-t') & 0 \\ \dot{\gamma}(t-t') & 1 & 0 \\ 0 & 0 & 1 \end{vmatrix}. \quad [10]$$

The invariants of $C_t^{-1}(t')$ in terms of the relative shear deformation $\gamma(s) = \dot{\gamma} \cdot s$ are

$$\begin{aligned} I_1 &= I_2 = 3 + \dot{\gamma}^2 s^2 \\ I_3 &= 1, \end{aligned} \quad [11]$$

where s is defined as $(t - t')$.

The following damping function $h(I_1, I_2) = h(\dot{\gamma}^2)$ has been successfully used in the description of stress and normal stress overshoot upon sudden start-up of steady flow of a low-density polyethylene melt (12):

$$h(\dot{\gamma}^2) = \exp[-n\sqrt{\dot{\gamma}^2 s^2}]. \quad [12]$$

The damping constant n , describing the non-linearity of the model, is correlated with the shear strains γ_s and γ_n , which correspond to maximum shear stress and maximum first normal stress difference respectively, by

$$n = \frac{1}{\gamma_s} = \frac{1}{\gamma_n}. \quad [13]$$

From [8], [10], and [12] the time-dependent shear viscosity $\eta(\dot{\gamma}, t)$ and primary normal stress function $\theta(\dot{\gamma}, t)$ are given by

$$\eta(\dot{\gamma}, t) = \int_0^t G(s) \exp[-n\sqrt{\dot{\gamma}^2 s^2}] \cdot (1 - n\sqrt{\dot{\gamma}^2 s^2}) ds, \quad [14]$$

and

$$\theta(\dot{\gamma}, t) = \int_0^t G(s) \exp[-n\sqrt{\dot{\gamma}^2 s^2}] \cdot (2 - n\sqrt{\dot{\gamma}^2 s^2}) ds. \quad [15]$$

By differentiation of eq. [14] with respect to $\dot{\gamma}$, the following relation can be found,

$$\theta(\dot{\gamma}, t) = -\frac{1}{n} \frac{\partial \eta(\dot{\gamma}, t)}{\partial \dot{\gamma}}, \quad [16]$$

which contains eq. [4] in the limit of steady state values:

$$\theta(\dot{\gamma}) = -\frac{1}{n} \frac{d\eta(\dot{\gamma})}{d\dot{\gamma}}. \quad [17]$$

If a finite series of exponential functions with amplitudes a_i and time constants τ_i is used for the relaxation modulus $G(t)$,

$$G(t) = \sum_i a_i \tau_i e^{-t/\tau_i}, \quad [18]$$

the values of $\eta(\dot{\gamma}, t)$ and $\theta(\dot{\gamma}, t)$ can be found by closed integration (24).

The steady state values are given by

$$\bar{\eta}(\dot{\gamma}) = \sum_i \frac{a_i \tau_i^2}{(1 + n \tau_i \dot{\gamma})^2}, \quad [19]$$

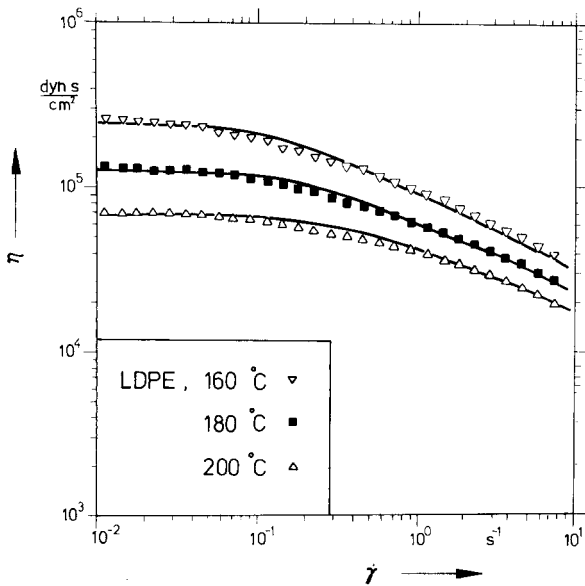


Fig. 1. Viscosity function η of low-density polyethylene melt (data of Chen and Bogue (7)):

∇ : 160°C
 \blacksquare : 180°C
 \triangle : 200°C.

Full curves: best fits by Carreau's viscosity equation (eq. [21])

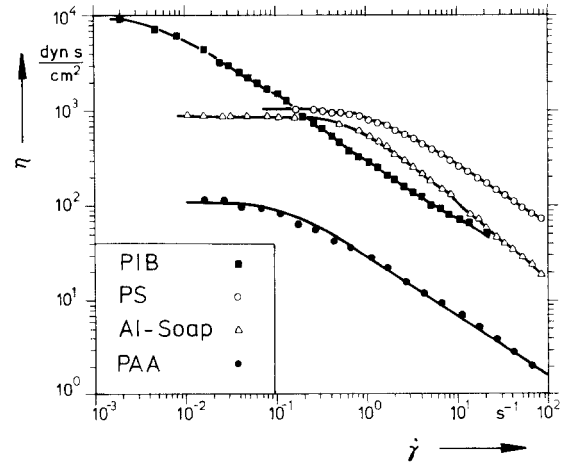


Fig. 3. Viscosity function η of three polymer solutions and a soap solution:

\blacksquare : 2% polyisobutylene (data of Huppler et al. (10)),
 \circ : 5% polystyrene (data of Ashare (11)),
 \bullet : 0.75% polyacrylamide (data of Marsh (9)),
 \triangle : 7% aluminium-soap (data of Huppler et al. (10)).

Full curves: best fits by Carreau's viscosity equation (eq. [21])

and

$$\theta(\dot{\gamma}) = 2 \sum_i \frac{a_i \tau_i^3}{(1 + n \tau_i \dot{\gamma})^3} \quad [20]$$

3. Data analysis: Carreau's viscosity equation

The shear viscosity function η for six polymer melts, three polymer solutions and an aluminium soap solution are shown in figs. 1 to 3. The solid lines are best fits of Carreau's viscosity equation (25),

$$\frac{\eta - \eta_\infty}{\eta_0 - \eta_\infty} = [1 + (\lambda \dot{\gamma})^2]^{-N}, \quad [21]$$

to the experimental data as obtained by Bird et al. (3). The parameter values of the fluids considered are given in table 1. η_0 is the zero shear viscosity, η_∞ the viscosity of the solvent, and λ a time constant. For the case of $\eta_\infty \ll \eta_0$, the slope of the viscosity function for high shear rates ($\lambda \dot{\gamma} \gg 1$) is equal to $-2N$ on a log-log plot and N is related to the power law exponent m in

$$\eta = \Phi \dot{\gamma}^{m-1} \quad [22]$$

by

$$N = (1 - m)/2. \quad [23]$$

From eqs. [4] and [21], the primary normal stress function θ is readily obtained,

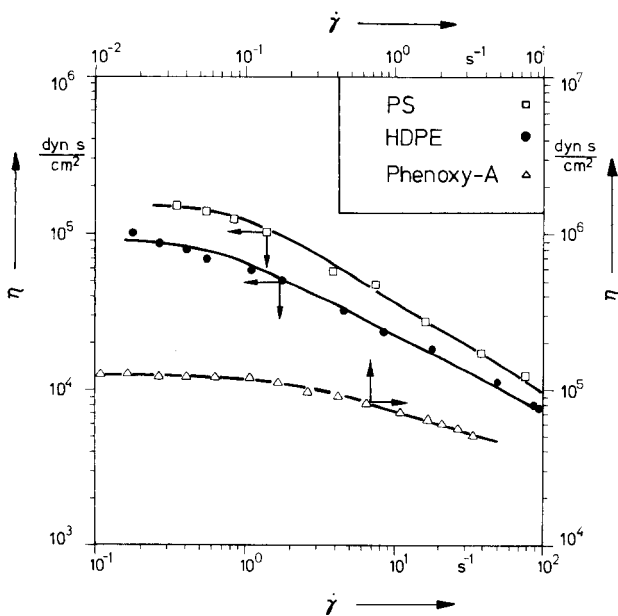


Fig. 2. Viscosity function η of three polymer melts:

\square : polystyrene, 180°C (data of Ballenger et al. (8)),
 \bullet : high-density polyethylene, 160°C (data of Ballenger et al. (8)),
 \triangle : phenoxy-A, 212°C (data of Marsh (9)).

Full curves: best fits by Carreau's viscosity equation (eq. [21])

Table 1. Properties of test fluids

Fluid	Ref.	T (°C)	Carreau's viscosity equation parameters				damping constant n (-)
			η_0 (dyn s/cm ²)	η_∞ (dyn s/cm ²)	λ (s)	N (-)	
<i>Polymer melts</i>							
Low-density polyethylene	7	160	$2.32 \cdot 10^5$	0	7.18	0.240	0.13
Low-density polyethylene	7	180	$1.21 \cdot 10^5$	0	5.23	0.217	0.13
Low-density polyethylene	7	200	$6.43 \cdot 10^4$	0	2.86	0.207	0.13
High-density polyethylene	8	160	$8.92 \cdot 10^4$	0	1.58	0.252	0.20
Polystyrene	8	180	$1.48 \cdot 10^5$	0	1.04	0.301	0.20
Phenoxy-A	9	212	$1.24 \cdot 10^5$	0	7.44	0.136	0.18
<i>Solutions</i>							
2% Polyisobutylene in Primol 355	10	25	$9.23 \cdot 10^3$	1.50	191.0	0.321	0.15
5% Polystyrene in Aroclor 1242	11	25	$1.01 \cdot 10^3$	0.59	0.84	0.310	0.18
0.75% Polyacrylamide in 95-5 water-glycerine	9	25	$1.06 \cdot 10^2$	0.10	8.04	0.318	0.10
7W Aluminium-soap in decalin and m-cresol	10	25	$8.96 \cdot 10^2$	0.10	1.41	0.400	0.20

$$\frac{\theta}{\lambda(\eta_0 - \eta_\infty)} = \frac{2N}{n} \lambda \dot{\gamma} [1 + (\lambda \dot{\gamma})^2]^{-(N+1)}, \quad [24]$$

$$\theta = \frac{1-m}{n} \phi \dot{\gamma}^{m-2}. \quad [25]$$

or, in the limit of the power law

In figs. 4 to 6, the normalized primary stress function $\theta/\lambda(\eta_0 - \eta_\infty)$ is plotted versus the non-dimensional shear rate $\lambda \dot{\gamma}$. The solid lines

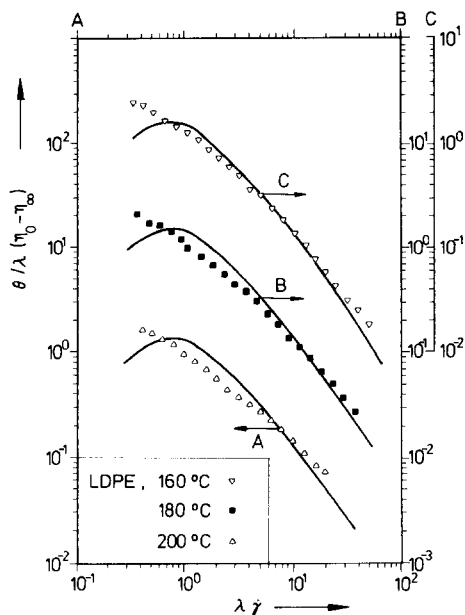


Fig. 4. Normalized primary stress function for low-density polyethylene melt (data of *Chen and Bogue* (7)): ∇ : 160°C, \blacksquare : 180°C, \triangle : 200°C.

Full curves: predicted values by eq. [24]

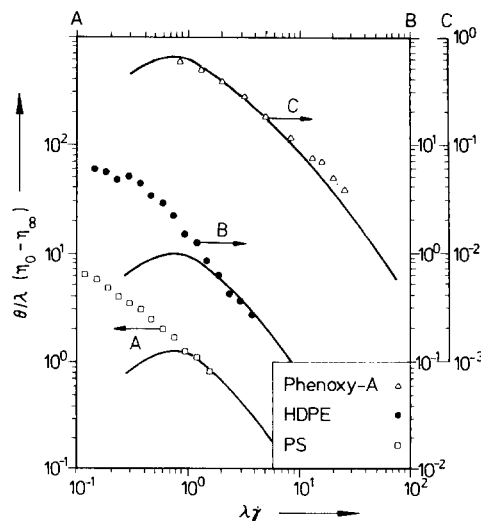


Fig. 5. Normalized primary stress function for three polymer melts:

\square : polystyrene, 180°C (data of *Ballenger et al.* (8)),
 \bullet : high-density polyethylene, 160°C (data of *Ballenger et al.* (8)),
 \triangle : phenoxy-A, 212°C (data of *Marsh* (9)).

Full curves: predicted values by eq. [24]

are obtained from eq. [24], where the parameter of non-linearity, n , has been adjusted in such a way as to give a best fit to the experimental data. The n -values used are listed in table 1, and lie between 0.13 and 0.2 for polymer melts and 0.1 and 0.2 for solutions. This agrees favourably with a damping constant of $n = 0.143$, which has been determined by a different method from stress and normal stress overshoot data of a low-density polyethylene melt (12).

As can be seen from figs. 4 to 6, agreement between predicted and measured values of the

Fig. 6. Normalized primary stress function for three polymer solutions and a soap solution:

■: 2% polyisobutylene (data of Huppler et al. (10)),
 ○: 5% polystyrene (data of Ashare (11)),
 ●: 0.75% polyacrylamide (data of Marsh (9)),
 △: 7% aluminium-soap (data of Huppler et al. (10)).

Full curves: predicted values by eq. [24]

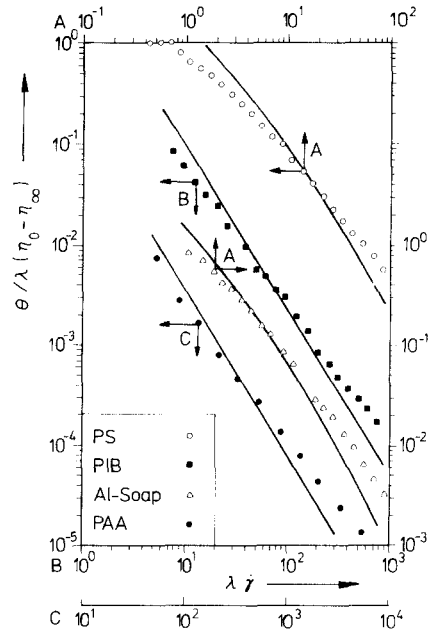


Table 2. Constants τ_i (s) and a_i (dyn/s cm²) of relaxation modulus $G(t)$ (eq. [18]) as determined from viscosity data of test fluids

Fluids	Ref.	T (°C)	τ_i	a_i	τ_i	a_i	τ_i	a_i	τ_i	a_i
<i>Polymer melts</i>										
Low-density polyethylene	7	160	10^2	$2.402 \cdot 10^0$	10^1	$1.821 \cdot 10^3$	10^0	$3.814 \cdot 10^4$	10^{-1}	$1.761 \cdot 10^6$
Low-density polyethylene	7	180	10^2	$1.579 \cdot 10^0$	10^1	$7.837 \cdot 10^3$	10^0	$3.430 \cdot 10^4$	10^{-1}	$9.327 \cdot 10^5$
Low-density polyethylene	7	200	10^2	$3.162 \cdot 10^{-1}$	10^1	$2.680 \cdot 10^2$	10^0	$3.137 \cdot 10^4$	10^{-1}	$4.523 \cdot 10^5$
High-density polyethylene	8	160	10^1	$6.851 \cdot 10^2$	10^0	$5.428 \cdot 10^4$	10^{-1}	$1.357 \cdot 10^6$	10^{-2}	$4.348 \cdot 10^7$
Polystyrene	8	180	10^1	$6.635 \cdot 10^2$	10^0	$1.194 \cdot 10^5$	10^{-1}	$2.075 \cdot 10^6$	10^{-2}	$6.289 \cdot 10^7$
Phenoxy-A	9	212	10^1	$6.070 \cdot 10^2$	10^0	$3.503 \cdot 10^4$	10^{-1}	$1.931 \cdot 10^6$	10^{-2}	$6.027 \cdot 10^7$
<i>Solutions</i>										
2% Polyisobutylene in Primol 355	10	25	10^3	$3.636 \cdot 10^{-3}$	10^2	$6.145 \cdot 10^{-1}$	10^1	$3.633 \cdot 10^{-1}$	10^0	$3.525 \cdot 10^2$
5% Polystyrene in Aroclor 1242	11	25	10^0	$9.382 \cdot 10^2$	10^{-1}	$1.261 \cdot 10^4$	10^{-2}	$4.910 \cdot 10^5$	10^{-3}	$7.071 \cdot 10^6$
0.75% Polyacrylamide in 95-5 water-glycerine	9	25	10^2	$1.037 \cdot 10^{-2}$	10^1	$6.231 \cdot 10^{-1}$	10^0	$8.593 \cdot 10^0$	10^{-1}	$3.999 \cdot 10^2$
7% Aluminium-soap in Decalin and <i>m</i> -Cresol	10	25	10^1	$1.796 \cdot 10^0$	10^0	$7.716 \cdot 10^2$	10^{-1}	$8.283 \cdot 10^1$	10^{-2}	$2.125 \cdot 10^5$

primary normal stress function is encouraging for $\lambda\dot{\gamma} \geq 1$, while for $\lambda\dot{\gamma} = 1/\sqrt{2N+1}$ a maximum of the primary normal stress function is predicted. This is due to the fact, that Carreau's viscosity equation prescribes a point of inflexion of the viscosity function at $\lambda\dot{\gamma} = 1/\sqrt{2N+1}$. To avoid any artificial effects in the prediction of the primary normal stress function, caused by the use of only one relaxation time in the description of the viscosity function as in the case of Carreau's viscosity equation, the exponential series approach will now be applied.

4. Finite series approach

A relaxation modulus $G(t)$ (eq. [18]) with five exponential terms was used and the steady state values of the viscosity function η and the primary normal stress function θ are given by eqs. [19] and [20].

Five relaxation times τ_i ($i = 1 \dots 5$) with decimal spacing were chosen (table 2). The amplitudes a_i were determined from the viscosity data by taking five discrete values $\eta(\dot{\gamma}_j)$ ($j = 1 \dots 5$) of the viscosity function at shear rates $\dot{\gamma}_j = 1/\tau_j$ and solving a system of five linear equations of the type

$$\eta(\dot{\gamma}_j) = \sum_{i=1}^5 \frac{a_i \tau_i^2}{(1 + n \tau_i \dot{\gamma}_j)^2}, \quad (j = 1 \dots 5). \quad [26]$$

The damping constant n was taken from table 1. The constants τ_i and a_i determined by this method are given in table 2 for the ten fluids considered.

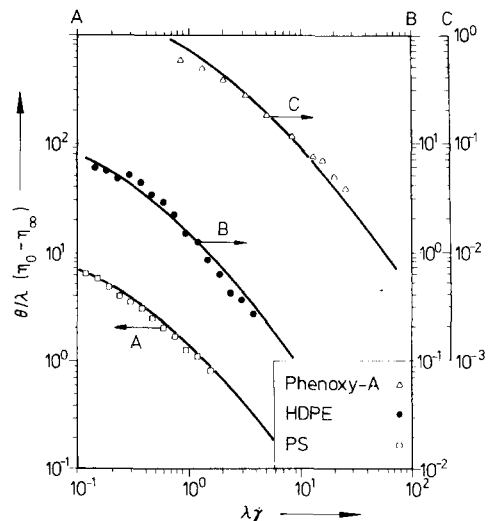


Fig. 8. Normalized primary stress function for three polymer melts:

□: polystyrene, 180°C (data of Ballenger et al. (8)),
 ●: high-density polyethylene, 160°C (data of Ballenger et al. (8)),
 △: phenoxy-A, 212°C (data of Marsh (9)).
 Full curves: predicted values by eq. [20]

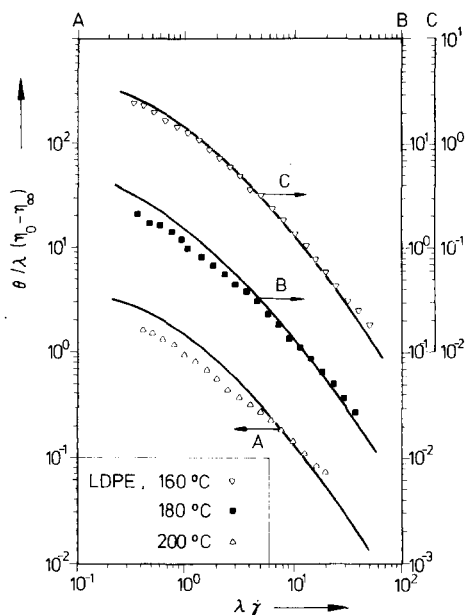


Fig. 7. Normalized primary stress function for low-density polyethylene melt (data of Chen and Bogue (7)):
 ▽: 160°C,
 ■: 180°C,
 △: 200°C.
 Full curves: predicted values by eq. [20]

The primary normal stress function was then calculated from eq. [20] and is shown in figs. 7 to 9. For high values of the non-dimensional shear rate $\lambda\dot{\gamma}$, predictions of the exponential series approach coincide with those of Carreau's viscosity equation, as expected. At low shear rates, however, agreement between predicted values of the primary normal stress function and experimental data is markedly improved, as in the case of the polystyrene and high-density polyethylene melt data (fig. 8).

5. Concluding remarks

It has been demonstrated that eq. [4], correlating viscosity and normal stress difference data, is a valid description of material behavior over a shear rate range of several orders of magnitude for the ten polymer melts and solutions considered. Despite the fact that these fluids are vastly different from one another,

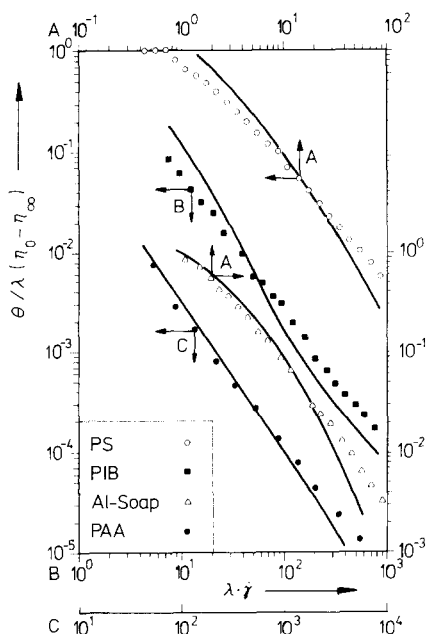


Fig. 9. Normalized primary stress function for three polymer solutions and a soap solution:

- : 2% polyisobutylene (data of Huppler et al. (10)),
 - : 5% polystyrene (data of Ashare (11)),
 - : 0.75% polyacrylamide (data of Marsh (9)),
 - △: 7% aluminium-soap (data of Huppler et al. (10)).
- Full curves: predicted values by eq. [20]

a single material parameter, the damping constant n , is sufficient for this correlation.

Care has to be taken when fitting the viscosity function for low shear rates ($\lambda \dot{\gamma} < 1$) by an empirical equation of Carreau's type (eq. [21]); inflexion points of the viscosity curve will give rise to artificial maxima in the predicted primary normal stress function.

Acknowledgements

The author wishes to express his gratitude to Prof. Dr.-Ing. G. Schenkel for helpful comments, and to Dr. Münstedt and Dr. Laun for valuable discussions. The financial support from the Deutsche Forschungsgemeinschaft is gratefully acknowledged.

Summary

Based on a single integral constitutive equation with a strain-dependent memory function, a relation between the primary normal stress function θ and the shear viscosity function η is proposed. According to this theory, the primary normal stress function θ can be obtained from viscosity data by simple differentiation of the viscosity function η with respect to the shear rate $\dot{\gamma}$, and multiplication by a factor $(-1/n)$. The material parameter n is thereby associated with the strain dependence of the memory function.

This relation was compared with the viscosity and primary normal stress data of six polymer melts, three polymer solutions, and an aluminium-soap solution, which were measured by several research groups and are available in the literature. In spite of the vast differences in physical constitution and chemical structure of the melts and solutions considered, agreement between predicted and measured values was encouraging.

Zusammenfassung

Ausgehend von einer Zustandsgleichung vom Integraltyp mit deformationsabhängiger Gedächtnisfunktion wird eine einfache Beziehung zwischen der ersten Normalspannungsfunktion θ und der Scherviskositätsfunktion η vorgeschlagen. Nach dieser Theorie kann man die erste Normalspannungsfunktion θ aus Viskositätsdaten erhalten, indem man die Viskositätsfunktion η nach der Schergeschwindigkeit $\dot{\gamma}$ ableitet und den entstehenden Ausdruck mit einem Faktor $(-1/n)$ multipliziert. Dabei hängt die Materialgröße n mit der Deformationsabhängigkeit der Gedächtnisfunktion zusammen.

Diese Beziehung wurde mit den Viskositäts- und Normalspannungsdaten von sechs Polymerschmelzen, drei Polymerlösungen und einer Aluminiumseifenlösung verglichen, die von verschiedenen Forschergruppen gemessen wurden und die in der Literatur verfügbar sind. Trotz der großen Unterschiede im physikalischen Zustand und in der chemischen Struktur der betrachteten Schmelzen und Lösungen wurde eine gute Übereinstimmung zwischen der Theorie und den experimentellen Daten gefunden.

References

- 1) Weissenberg, K., Proc. 1st Intern. Congr. Rheology, Vol. 3, p. 36 (Amsterdam 1949).
- 2) Criminale, W. O., J. L. Ericksen, G. L. Filbey, Arch. Rat. Mech. Anal. **1**, 410 (1957).
- 3) Abdel-Khalik, S. I., O. Hassager, R. B. Bird, Polym. Eng. Sci. **14**, 859 (1974).
- 4) Bird, R. B., O. Hassager, S. I. Abdel-Khalik, AIChE J. **20**, 1041 (1974).
- 5) Goddard, J. D., C. Miller, Rheol. Acta **5**, 177 (1966).
- 6) Landau, L. D., E. M. Lifshitz, Statistical Physics, p. 384–391 (London 1969).
- 7) Chen, I.-J., D. C. Bogue, Trans. Soc. Rheol. **16**, 59 (1972).
- 8) Ballenger, T. F., I.-J. Chen, J. W. Crowder, G. E. Hagler, D. C. Bogue, J. L. White, Trans. Soc. Rheol. **15**, 195 (1971).
- 9) Marsh, B. D. (1967) (as cited by P. J. Carreau, I. F. Macdonald, R. B. Bird, Chem. Eng. Sci. **23**, 901 (1968)).
- 10) Huppler, J. D., E. Ashare, L. A. Holmes, Trans. Soc. Rheol. **11**, 159 (1968).
- 11) Ashare, E., PhD thesis, University of Wisconsin (1968).
- 12) Wagner, M. H., Rheol. Acta **15**, 136 (1976).
- 13) Meissner, J. M., J. Appl. Polymer Sci. **16**, 2877 (1972).
- 14) Meissner, J. M., Rheol. Acta **14**, 201 (1975).

- 15) *Bernstein, B., E. A. Kearsley, L. J. Zapas*, *Trans. Soc. Rheol.* **7**, 391 (1963); *J. Res. Natl. Bur. Std.* **68**, 103 (1964).
- 16) *Kaye, A.*, College of Aeronautics, Note No. 134 (Cranfield 1962).
- 17) *Tanner, R. I., G. Williams*, *Trans. Soc. Rheol.* **14**, 19 (1970).
- 18) *Yen, H.-Ch., L. V. Mc Intire*, *Trans. Soc. Rheol.* **18**, 495 (1974).
- 19) *Lodge, A. S.*, *Elastic Liquids* (London-New York 1964).
- 20) *Lodge, A. S.*, *Body Tensor Fields in Continuum Mechanics* (London-New York 1974).
- 21) *Chang, H., A. S. Lodge*, *Rheol. Acta* **11**, 127 (1972).
- 22) *Lodge, A. S., J. M. Meissner*, *Rheol. Acta* **12**, 41 (1973).
- 23) *Wagner, M. H.*, *Rheol. Acta* **15**, 133 (1976).
- 24) *Laun, H. M.*, private communication (1975).
- 25) *Carreau, P. J.*, PhD thesis, University of Wisconsin (1968).

Author's address:

Dr.-Ing. Dipl.-Phys. *M. H. Wagner*
Institut für Kunststofftechnologie
Universität Stuttgart
Böblinger Straße 70
D-7000 Stuttgart 1 (BRD)

Present address:

Dr.-Ing. Dipl.-Phys. *M. H. Wagner*
c/o Prof. Dr. *J. M. Meissner*
Eidgenössische Technische Hochschule Zürich
Technisch-Chemisches Laboratorium
Universitätsstr. 6
CH-8006 Zürich (Switzerland)